Predictive Patterns of Glutamine Synthetase Immunohistochemical Staining in CTNNB1-mutated Hepatocellular Adenomas

Sempoux, Christine; Gouw, Annette S. H.; Dunet, Vincent; Paradis, Valerie; Balabaud, Charles; Bioulac-Sage, Paulette

Published in:
American Journal of Surgical Pathology

DOI:
10.1097/PAS.0000000000001675

Predictive Patterns of Glutamine Synthetase Immunohistochemical Staining in *CTNNB1*-mutated Hepatocellular Adenomas

Christine Sempoux, MD, PhD, Annette S.H. Gouw, MD, PhD,† Vincent Dunet, MD,‡ Valérie Paradis, MD, PhD,§ Charles Balabaud, MD,‖ and Paulette Bioulac-Sage, MD‖*

Abstract: Some hepatocellular adenoma (HCA) subtypes are characterized by different *CTNNB1* mutations, leading to different beta-catenin activation levels, hence variable immunostaining patterns of glutamine synthetase (GS) expression, and different risks of malignant transformation. In a retrospective multicentric study of 63 resected inflammatory (n = 33) and noninflammatory (n = 30) molecularly confirmed *CTNNB1*-mutated b-(I)HCA, we investigated the predictive potential of 3 known GS patterns as markers for *CTNNB1* exon 3, 7/8 mutations. Pattern 1 (diffuse homogenous) allowed recognition of 17/21 exon 3 non-S45 mutated b-(I)HCA. Pattern 2 (diffuse heterogenous) identified all b-(I)HCA harboring exon 3 S45 mutation (20/20). Pattern 3 (focal patchy) distinguished 12/22 b-(I)HCA with exon 7/8 mutations. In exon 3 S45 and 7/8 mutations, both b-HCA and b-IHCA showed a $GS^+/CD34^-$ rim with diffuse CD34 positivity in the center of the lesion. Interobserver reproducibility was excellent for exon 3 mutations. Comparative analysis of GS patterns with molecular data showed 83% and 80% sensitivity (b-HCA/b-IHCA) and 100% specificity for exon 3 non-S45. For exon 3 S45, sensitivity was 100% for b-(I)HCA, and specificity 93% and 92% (b-HCA/b-IHCA). For exon 7/8, sensitivity was 55% for both subtypes and specificity 100% and 96% (b-HCA/b-IHCA). Preliminary data from 16 preoperative needle biopsies from the same patients suggest that this panel may also be applicable to small samples. In surgically resected HCA, 2 distinct GS patterns can reliably predict *CTNNB1* exon 3 mutations, which are relevant because of the higher risk for malignant transformation. The third pattern, although specific, was less sensitive for the identification of exon 7/8 mutation, but the $GS^+/CD34^-$ rim is a valuable aid to indicate either an exon 3 S45 or exon 7/8 mutation.

From the *Service of Clinical Pathology, Institute of Pathology; ‡Department of Diagnostic and Interventional Radiology, Lausanne University Hospital and University of Lausanne, Lausanne, Switzerland; †Department of Pathology and Medical Biology, University Medical Center Groningen, Groningen, The Netherlands; §Department of Pathology, Beaujon Hospital, Clichy; and ‖Bordeaux University, INSERM, BaRITOn, U1053, Bordeaux, France.

C.S. and A.S.H.G. contributed equally.

Conflicts of Interest and Source of Funding: The authors have disclosed that they have no significant relationships with, or financial interest in, any commercial companies pertaining to this article.

Correspondence: Christine Sempoux, MD, PhD, Service of Clinical Pathology, Institute of Pathology, Lausanne University Hospital, Rue du Bugnon 25, Lausanne 1011, Switzerland (e-mail: christine.sempoux@chuv.ch).

Key Words: beta-catenin–activated hepatocellular adenoma, beta-catenin–activated inflammatory hepatocellular adenoma, CD34, glutamine synthetase, hepatocellular adenoma, immunohistochemistry, inflammatory hepatocellular adenoma, molecular analysis

(*Am J Surg Pathol* 2021;45:477–487)

Hepatocellular adenomas (HCAs) are rare, benign hepatocellular neoplastic lesions, predominantly occurring in female patients in their reproductive age, usually after prolonged use of oral contraception.[1] The 2 major complications of HCA are hemorrhage and malignant transformation, developing in 15% to 25%[2,3] and 5% to 8%[2,4–7] of the cases, respectively. HCAs are molecularly categorized in different genotypes and the subsequent altered expression of several proteins in the tumor provides the possibility to recognize HCA subtypes using immunohistochemical (IHC) analyses.[7] Malignant transformation of HCA in hepatocellular carcinoma (HCC) is more frequent in men[2] and in some clinical contexts such as vascular liver diseases,[8] androgen consumption,[9] or metabolic disorders.[10] It also depends on mutations in the *CTNNB1* gene.[11]

There are different types of *CTNNB1* mutations in HCA, leading to variable levels of beta-catenin activation, hence to different levels of increased risk of malignant transformation.[1] Mutations in exon 3 of the *CTNNB1* gene, leading to a strong activation of the Wnt/beta-catenin pathway, are associated with a high risk for the development of HCC, whereas mutations in exons 7 and 8 display low risk of malignant transformation.[2] Both the recognition of a *CTNNB1* mutation in HCA and correct identification of the type of mutation are relevant for clinical management, as imaging is as yet unable to recognize such subtypes. Molecular analysis of tumor tissue samples both on frozen[4] and on formalin-fixed paraffin-embedded (FFPE) materials[12,13] is not as widely available in routine practice as IHC, and if the technique is available, the molecular analysis does not always include *CTNNB1* exons 7 and 8 mutations.

Nuclear beta-catenin expression, the IHC hallmark of exon 3 *CTNNB1* mutation, is regarded as an inadequate marker for beta-catenin activation because of its low sensitivity, in contrast with the recognized suitability of glutamine synthetase (GS), a target protein of the

CTNNB1 gene, as a surrogate IHC marker for beta-catenin mutation.[7,14] Several studies have documented patterns of GS IHC expression that seem to distinguish the different *CTNNB1* mutations.[11,15,16] However, the lack of consensus on the terminology of the different GS staining patterns and on the criteria for their application and interpretation impedes a standardized and common application of GS as a predictive marker for *CTNNB1* mutations in HCA.[17,18] In addition, it is still unclear whether the GS immunostaining pattern is similar in beta-catenin–mutated hepatocellular adenoma (b-HCA) and beta-catenin–mutated inflammatory hepatocellular adenoma (b-IHCA) when harboring the same type of *CTNNB1* mutation.

The current study was undertaken to address these issues, by the evaluation of specific patterns of GS IHC expression associated with exons 3, 7, and 8 *CTNNB1* mutations in b-HCA and b-IHCA. We studied the predictive value of GS immunostaining as a marker of *CTNNB1* mutations and established its potentials and limitations for routine practice. In addition, we assessed the additional and complementary role for CD34, which had only been described in a few case reports and reviews.[15,19,20] In particular, we evaluated the role of a $GS^+/CD34^-$ rim at the periphery of the tumor, previously observed in HCA with exon 3 S45 and exon 7/8 mutations.[21] Only b-HCA and b-IHCA subtypes were included because the incidence and consequences of *CTNNB1* mutations in these 2 subgroups of HCA are well established, which is not the case in the other subtypes. Although it has been shown that HNF1α-inactivated HCA[22] or sonic-hedgehog HCA[23] can undergo malignant transformation, there is so far no identified role for *CTNNB1* in these subtypes; hence, the interpretation of GS staining in that context should be made with caution. We included inflammatory hepatocellular adenoma (IHCA) as controls, for comparison with b-IHCA. In this study, we follow the concept, which we regard as mandatory for routine practice, that the diagnosis and subtyping of HCA should be performed using conventional hematoxylin and eosin staining and ancillary immunohistology[7] before proceeding to the interpretation of GS expression.

MATERIALS AND METHODS

This is a retrospective multicentric study of 111 surgically resected b-HCA, b-IHCA, and IHCA, collected from 4 departments of Pathology: CHU Bordeaux (Bordeaux, France, 76 cases), University Medical Center Groningen (Groningen, The Netherlands, 8 cases), Beaujon Hospital (Paris, France, 5 cases), and Lausanne University Hospital (Lausanne, Switzerland, 4 cases). In all the centers, patients had been informed and/or given their consent for using their anonymized data for scientific purposes.

Inclusion was based on the availability of the following elements. It was mandatory to have the molecular data of *CTNNB1* mutations of exons 3, 7, and 8 as the gold standard, performed on frozen or FFPE tissues. Mutations in exon 3 were differentiated in mutations at the hotspot S45 on one side, and other mutations or deletion referred as "exon 3 non-S45" on the other side. Exons 7 and 8 mutations were pooled in the same group. IHC of C-reactive protein and/or serum amyloid A was available in all cases to recognize IHCA and b-IHCA. GS and CD34 IHC were evaluated on samples containing the interface between lesional and nonlesional liver tissue. HCA with extensive hemorrhage or necrosis were excluded, except if there was an area of enough viable tissue. In case of an existing associated HCC, only the HCA part was studied. The IHC techniques and applied antibodies have been described previously[14] and are fully comparable in the 4 participating centers.

The observers assessed all cases individually and were blinded to the clinical and mutational data. Individual microscopic analysis was preceded by a short introduction organized as a joint histologic session at the multihead microscope using 10 cases to reach an agreement regarding the different patterns of GS staining, derived from the work of Rebouissou et al,[11] and is depicted in Figure 1.

Pattern 1, the *diffuse homogenous GS pattern*, corresponds to a diffuse, moderate to strong, GS expression in all lesional hepatocytes, often associated with the presence of various numbers of beta-catenin positive nuclei and an increased but non diffuse CD34 staining of the sinusoids. Molecularly, this pattern had been associated with either large deletions or mutations in exon 3 (outside the hotspot S45) of the *CTNNB1* gene, corresponding mainly to T41 or D32-S37 mutations.[11]

Pattern 2, the *diffuse heterogenous GS pattern*, shows GS expression of variable intensity in a majority of individual hepatocytes distributed diffusely in the entire lesion, giving a "starry sky" impression, at lower power.[7] In addition, a strong GS^+ but $CD34^-$ rim is seen at the border of the HCA, with a contrasting diffuse positive CD34 expression in the center of the lesion. None or just a few beta-catenin positive nuclei were found. This second type of IHC pattern had been associated with *CTNNB1* exon 3 S45 mutation.[11]

Pattern 3, the *focal patchy GS pattern*, is characterized by a faint GS staining in few hepatocytes irregularly scattered within the HCA, often associated with a variable number of GS^+ patches of predominantly perivenular hepatocytes. This pattern is again associated with a $GS^+/CD34^-$ rim at the border between the HCA and the normal liver, and with the same contrasting feature of diffuse CD34 positivity in the center. Nuclear beta-catenin positivity was absent. This pattern had been associated with exon 7 or 8 *CTNNB1* K335 or N387 point mutations.[11]

Absence of *CTNNB1* mutations is associated with absence of GS expression, except around some veins or occasional patches within the HCA or at its periphery, with absence of a well-defined GS rim. CD34 expression is unremarkable.

The algorithm describing the different staining patterns corresponding to the *CTNNB1* mutations presented in Figure 2 summarizes the scoring workflow used for this study. For each case, the evaluation started by subtyping the HCA into IHCA or non-IHCA, according to the C-reactive protein

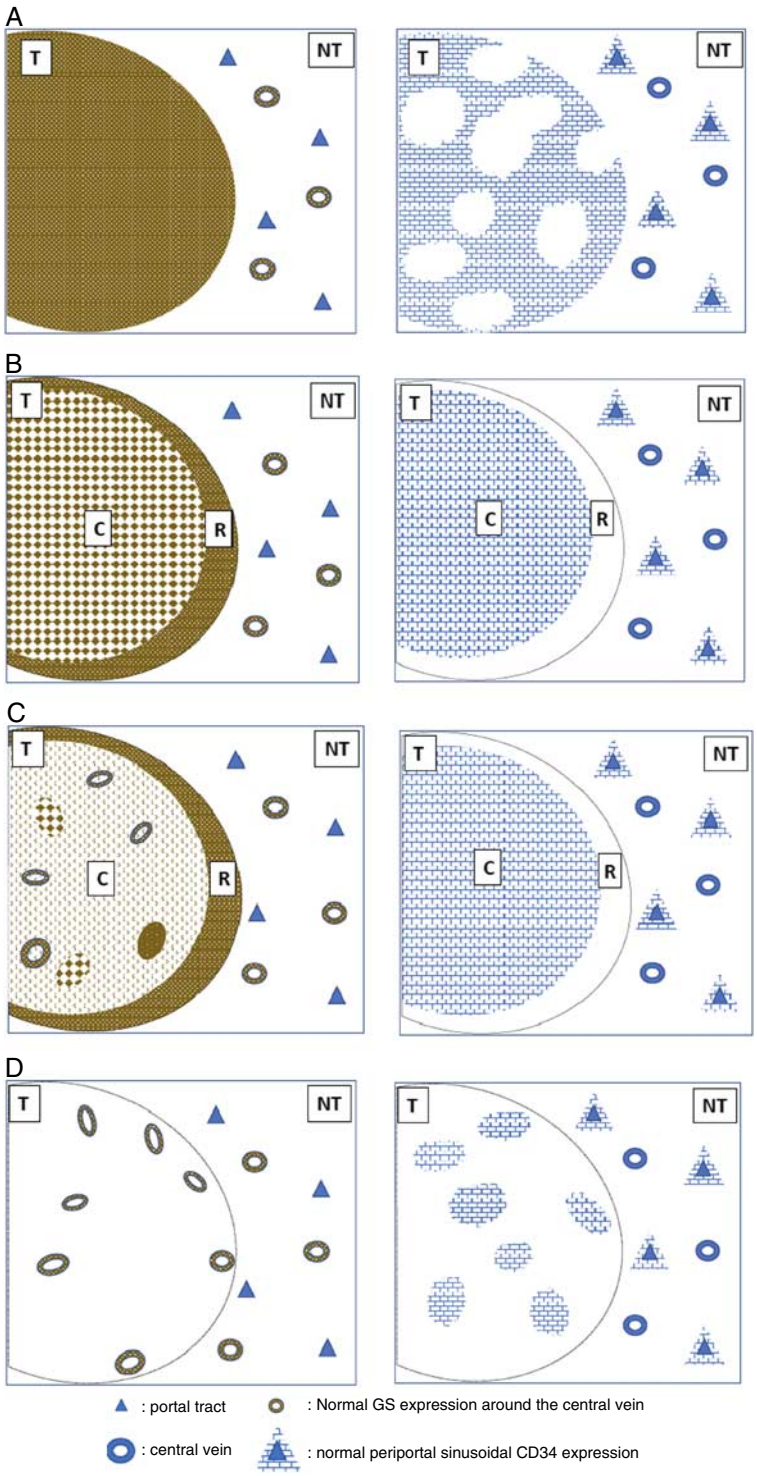

FIGURE 1. The different hepatocellular GS (brown, left panel) and sinusoidal CD34 (blue, right panel) patterns of staining. A, Pattern 1: diffuse homogenous GS expression and increased but non diffuse sinusoidal CD34 expression in the tumor. B, Pattern 2: diffuse heterogenous GS expression; $GS^+/CD34^-$ rim and diffuse sinusoidal CD34 expression in the center of the tumor. C, Pattern 3: focal patchy GS expression pattern; $GS^+/CD34^-$ rim and diffuse sinusoidal CD34 expression in the center of the tumor. D, IHCA without *CTNNB1* mutation showing variable perivascular GS expression in the tumor and unremarkable CD34 expression. In the non tumoral liver, there is a normal perivenular GS expression around the central veins and a periportal sinusoidal expression of CD34. C indicates center of the tumor; NT, non tumoral liver; R, rim within the HCA, at the margin between tumoral and non tumoral liver; T, tumor (HCA).

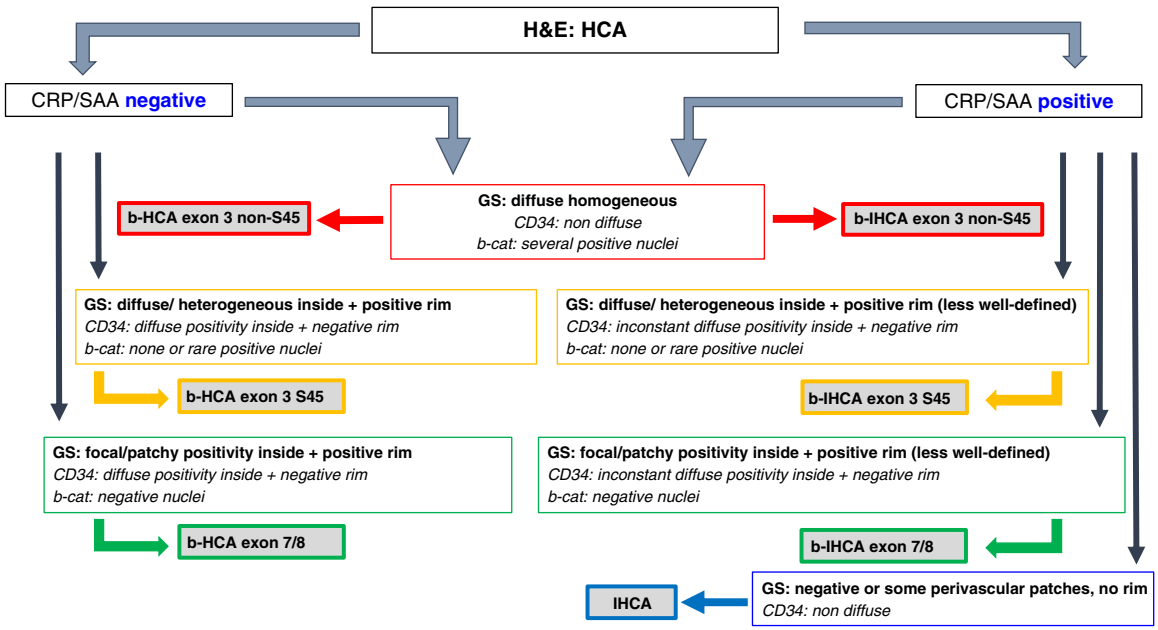

FIGURE 2. Algorithm used in this study, applicable in routine practice. CRP/SAA indicates C-reactive protein and/or serum amyloid A; H&E, hematoxylin and eosin.

and/or serum amyloid A immunostaining followed by the evaluation of GS, beta-catenin, and CD34 immunostainings. After individual evaluations of all cases, discordant results were discussed at the multihead microscope to reach a final consensus, still blinded to the molecular results to assess the interobserver reproducibility. Hereafter, the conclusions were reconciled with the molecular data to define the sensitivity and specificity of the 3 GS IHC patterns of staining.

Statistical Analysis

All statistics were performed using the Stata 13.1 software (StataCorp, College Station, TX). Continuous variables are displayed as mean ± SD and categorical variables as number or percentage. Interobserver reproducibility between the readers was tested for the 7 subtypes defined by molecular analysis. To this purpose, we used the unweighted Gwet AC1 coefficient corrected for chance agreement to overcome the 2 paradoxes of the Cohen κ, that is, (1) low κ despite high agreement under highly symmetrical imbalanced marginals and (2) higher κ values for asymmetrical imbalanced marginal distributions.[24,25] We used a modified Landis and Koch scale to characterize the value of Gwet AC1 coefficient, as follows: poor when Gwet AC1 was <0.00, slight between 0.00 and 0.20, fair between 0.21 and 0.40, moderate between 0.41 and 0.60, good between 0.61 and 0.80, and excellent above 0.81. Finally, the diagnostic performance of consensus was evaluated by calculating the sensitivity, specificity, positive and negative predictive values, and area under the curve with respective 95% confidence interval (CI) for each subtype considering molecular analysis as the gold standard. A P-value < 0.05 was considered statistically significant.

RESULTS

Ninety-three HCA samples from 87 patients (11 men, age range: 14 to 59 y, median: 35 y; 76 women, age range: 19 to 66 y, median: 33 y) fitted the inclusion criteria (Table 1). One woman who had 3 HCAs and 4 women who had 2 HCAs were included in the series. Sixty-three samples were IHCA (33 b-IHCA and a control group of 30 IHCA) and 30 were b-HCA. On the basis of molecular data, 15/33 b-IHCA samples had *CTNNB1* exon 3 non-S45 mutation, 7 samples had exon 3 S45 mutation, and 11 samples had exon 7 or 8 mutations. Of the 30 b-HCA samples, 6 had exon 3 non-S45 mutation, 13 had exon 3 S45 mutation, and 11 samples had exon 7 or 8 mutation (Table 1). Four cases were associated with an existing HCC (2 b-HCA exon 3 non-S45, 1 b-HCA exon 3 S45, and 1 b-IHCA exon 3 non-S45). In 3 of these 4 cases and in 6 additional cases (2 b-HCA exon 3 non-S45, 1 b-HCA exon 3 S45, 2 b-IHCA exon 3 non-S45, and 1 b-IHCA exon 3 S45), the HCAs showed some focal cytoarchitectural atypia yet insufficient to reach the diagnosis of HCC. None had *TERT* promoter mutation.

Pattern 1: Diffuse Homogenous GS Pattern

This pattern allowed recognition of 5/6 b-HCA and 12/15 b-IHCA with *CTNNB1* exon 3 non-S45 mutation with an excellent interobserver reproducibility (AC1 values of 0.87 [95% CI: 0.48-1.0] for b-HCA and 0.90 [95% CI: 0.74-1.0] for b-IHCA). There was an excellent sensitivity of 83% (95% CI: 36$-99%) for b-HCA and 80% (95% CI: 52%-96%) for b-IHCA, whereas the specificity rate was 100% (95% CI: 95%-100%) for both types. The GS staining intensity was strong (Fig. 3A). CD34 staining was increased but never diffuse (Fig. 3B). Scattered beta-catenin positive nuclei were

TABLE 1. Cases of the Series, Grouped by Molecular Categories

Sample	Age/ Sex	n/Size (cm) (Specific Etiology)	IHC Diagnosis Right/Discordance According to MA
b-HCA exon 3 non-S45 (N = 6)			
42 (T41)*	42/M	1n/10	Discordance (S45)
59 (D32-S37)*	14/M	Several n/2.7 (androgens)	Right
66 (large deletion)*	35/F	1n/12.5	Right
68	20/F	1n/5	Right
78 (large deletion)*	66/F	1n/6	Right
105 (large deletion)*	18/M	Adenomatosis/3.8 (glycogenosis type 1)	Right
b-HCA exon 3 S45 (N = 13)			
11	38/F	1n/6	Right
14	29/F	1n/9	Right
18	23/F	1n/5.5	Right
24†	28/F	1n/16	Right
30*	28/F	1n/5	Right
41*	24/F	1n/8	Right
47*	21/F	1n/9	Right
54*	29/F	1n/14	Right
61*	21/F	1n/10	Right
72	28/F	1n/5.5	Right
76	46/F	1n/15	Right
92*†	28/F	1n/15	Right
108	24/F	1n/5.2	Right
b-HCA exon 7/8 (N = 11)			
20	34/F	1n/7	Right
26*	22/F	1n/13	Right
29	29/F	1n/8	Right
43†	28/F	1n/2.8	Discordance (S45)
56*	28/F	1n/5	Discordance (S45)
70	30/F	5n/7	Right
77†	24/F	3n/3	Discordance (S45)
80	26/F	1n/5	Right
88*	27/F	1n/11	Discordance (S45)
90 Lausanne	23/F	1n/20	Discordance (S45)
91*	24/F	1n/8	Right
b-IHCA exon 3 non-S45 (N = 15)			
1 (deletion)	23/F	1n/11	Right
8 (large deletion)*	32/M	1n/3.5	Right
9 (T41)*	35/F	4n/7	Right
13 T2 (T41)	33/F	2n/1.8	Discordance (S45)
21	27/M	1n/7 (FAPC)	Right
22 T4 (A39G)*	46/F	4n/1.5	Discordance (S45)
35 T1 (A39G)* (*same as case 22*)	46/F	4n/10	Right
38 (P52S)	46/F	1n/7	Discordance (S45)
39 (D32-S37)*	35/F	1n/3	Right
51 (T41)*	26/F	1n/3.5	Right
52 (large deletion)*	59/M	1n/13	Right
63 T2 (T41)*	44/F	I-adenomatosis/ 4.2	Right
83 (T41)*	38/F	4n/7	Right
96 (T41)*	49/M	1n/3.5	Right
98 (T41)*	35/M	1n/5.5	Right
b-IHCA exon 3 S45 (N = 7)			
10	40/F	1n/5	Right
28	35/F	1n/4	Right
32*	45/F	I-adenomatosis/7	Right
82*	29/F	several n/5	Right
106*	34/F	1n/8.3	Right
107	36/F	1n/8	Right
109	21/F	1n/10.5	Right
b-IHCA exon 7/8 (N = 11)			
3*	46/F	1n/6	Right
5*	35/F	1n/10	Right
12 (T1) (*same as case 13*)	33/F	2n/4.4	Discordance (IHCA)
17*	53/M	1n/7	Discordance (S45)
19*	34/F	1n/8	Right
65*	42/F	1n/5	Discordance (IHCA)
69*	50/M	1n/10	Discordance (S45)
71*	28/M	1n/4	Right
74*	51/F	1n/11	Right
75*	41/F	1n/4	Discordance (S45)
81	19/F	1n/13	Right
IHCA (N = 30)			
2	34/F	I-adenomatosis/9	Right
6	46/F	I-adenomatosis/ 5.5	Right
7	45/F	I-adenomatosis/9	Right
23 (T3) (*same as cases 22, 35*)	46/F	I-adenomatosis/3	Right
27	53/F	1n/15	Discordance (b-IHCA 7/8)
33	54/F	1n/8	Right
37 (T3)	51/F	I-adenomatosis/ 3.3	Right
40 (T4) (*same as case 37*)	51/F	I-adenomatosis/4	Right
44	33/M	1n/8	Right
48 (T1)	41/F	I-adenomatosis/7	Right
49 (T2) (*same as case 48*)	41/F	I-adenomatosis/2	Right
50	48/F	1n/6	Discordance (b-IHCA 7/8)
53	27/F	4n/6	Right
57	24/F	1n/8	Right
62	31/F	1n/9	Discordance (b-IHCA exon 3 S45)
64	30/F	1n/10	Right
67	36/F	1n/10	Right
79	33/F	1n/1.5	Right
84 (T2) (*another nodule was shHCA*)	31/F	3n/6	Right
87	42/F	1n/3	Right
89	50/F	3n/4 (systemic amyloidosis)	Right
93	27/F	2/8.7	Right
94	50/F	1n/13.5	Right
95	47/F	1n/14	Discordance (b-IHCA 7/8)
97	21/F	1n/15	Right
99	43/F	I-adenomatosis/5	Right
101	26/F	1n/13	Right
102	26/F	1n/14	Right
103	40/F	I-adenomatosis/5	Right
104 (*same as case 27; another n 2 y later*)	53/F	1n/3.5	Right

*Beta-catenin mutation/deletion according to data from Rebouissou et al.[11]

†Pregnancy cases with severe hemorrhage and HCA rupture.

Different HCA from the same surgical specimen (except case 104) are shown in italics.

Adenomatosis indicates > 10 HCA present on the surgical specimen (including microadenomas <1 cm); F, female; FAPC, familial adenomatosis polyposis coli; I-adenomatosis, inflammatory adenomatosis; M, male; MA, molecular analysis; n, number of HCA present on the surgical specimen; several, number of HCA > 4 <10 present on the surgical specimen; shHCA, sonic-hedgehog HCA; size (cm), of the HCA reviewed in this study.

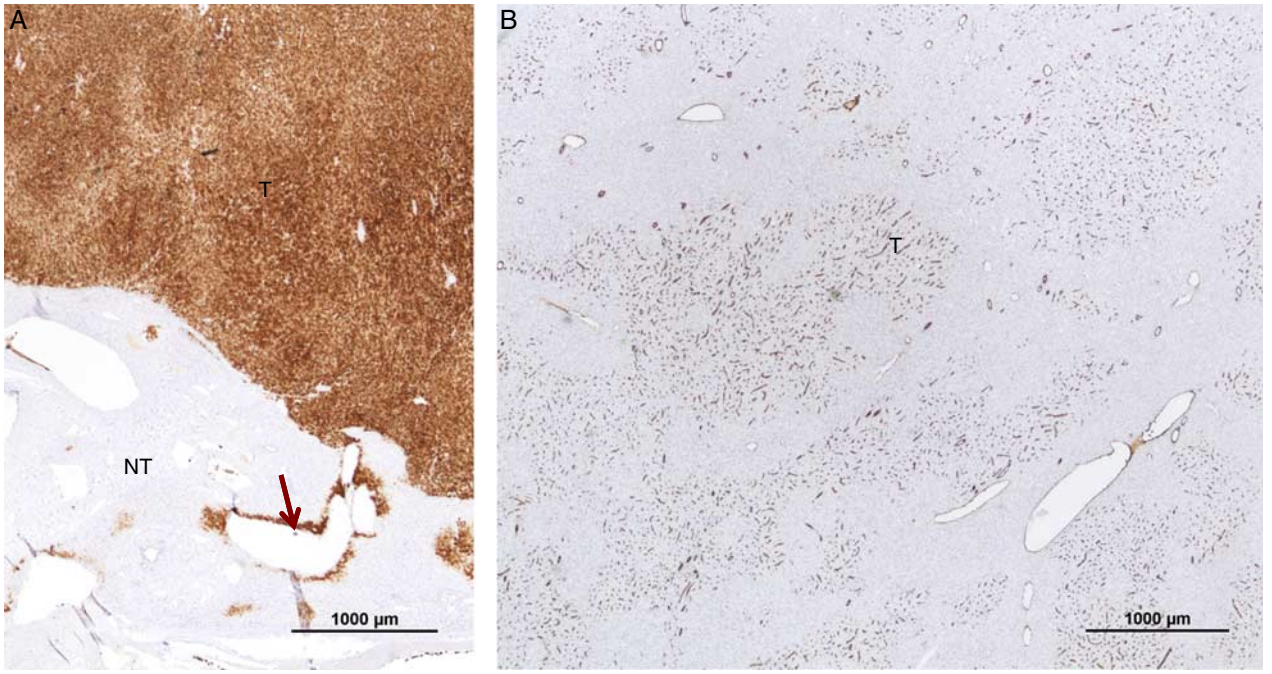

FIGURE 3. Pattern 1: diffuse homogenous GS pattern. A and B, Case 66 (b-HCA exon 3 non-S45, large deletion). A, Strong, homogenous, and diffuse expression of GS in the tumor (T), contrasting with the normal expression in non tumoral liver (NT) limited to a few hepatocytes around central veins (arrow). B, Sinusoidal expression of CD34 is increased but not diffuse in the T.

found but were not applied as a key decision-making feature. In this group, there were no differences in the GS and CD34 patterns between b-HCA and b-IHCA. In the group of 21 HCA harboring an underlying *CTNNB1* exon 3 non-S45 mutation, 1 b-HCA case and 3 b-IHCA cases were wrongly interpreted as having an exon 3 S45 mutation because of some heterogeneity in the intensity of GS staining at lower power.

Pattern 2: Diffuse Heterogenous GS Pattern

This GS pattern, associated with diffuse CD34 staining in the center of the lesion, and a strong $GS^+/CD34^-$ rim at the lesional border area, allowed a perfect recognition of the 13/13 b-HCA and 7/7 b-IHCA cases with *CTNNB1* exon 3 S45 mutation (Figs. 4A–D). Interobserver reproducibility was excellent (AC1 values of 0.96 [95% CI: 0.87-1.0] for b-HCA and 0.89 [95% CI: 0.58-1.0] for b-IHCA). This pattern and the rim proved to be highly sensitive (100% [95% CI: 59%-100%] for both types of HCA). A 93% (95% CI: 84%-97%) specificity rate was reached for b-HCA and 92% (95% CI: 84%-97%) for b-IHCA. Intensity of GS staining within the HCA was variable (Figs. 4E–G), which did not impede the recognition of the pattern. In b-IHCA, the rim was sometimes less well defined, and CD34 in the center was not always as diffuse as in b-HCA. The excellent sensitivity reflects that all cases containing exon 3 S45 mutation were correctly detected. The slightly less specificity results from wrongly diagnosed cases: 1 b-HCA and 3 b-IHCA exon 3 non-S45 (described in the previous paragraph), 5 b-HCA and 3 b-IHCA exon 7/8, and 1 IHCA (see below).

Pattern 3: Focal Patchy GS Pattern

This pattern, accompanied by a $GS^+/CD34^-$ rim and a diffuse CD34 expression in the center, identified 6/11 b-HCA and 6/11 b-IHCA with *CTNNB1* exon 7/8 mutations (Figs. 5A–D). A moderate interobserver reproducibility was reached for b-HCA (AC1 = 0.46, 95% CI: −0.03 to 0.96), whereas it was good for b-IHCA (AC1 = 0.67, 95% CI: 0.35-0.98). The sensitivity of the criteria for the identification of b-HCA exon 7/8 was 55% (95% CI: 23%-83%) with a 100% (95% CI: 96%-100%) specificity. For b-IHCA, the sensitivity was also 55% (95% CI: 23%-83%) with a 96% (95% CI: 90%-99%) specificity. In contrast with b-HCA, b-IHCA with exon 7/8 mutation often showed a less well-defined rim, and larger perivascular GS^+ areas in the tumoral center. Five b-HCA and 3 b-IHCA were wrongly considered as having exon 3 S45 mutations (see previous paragraph), and 2 b-IHCA were considered as IHCA. In addition, 3 IHCA were wrongly interpreted as b-IHCA exon 7/8 mutation (see below).

One additional observation made in case of *CTNNB1* exon 3 S45 and exon 7/8 mutations, in b-HCA more often than in b-IHCA, was the presence of a focal increase in large irregular vessels in the $CD34^+$ area, usually not far from the rim.

IHCA Without *CTNNB1* Mutation

All but 4 of 30 IHCA cases were correctly interpreted as devoid of *CTNNB1* mutation. GS expression was negative in most cases, with mainly some perivascular expression in comparable extents as in the nonlesional counterpart, or slightly increased, at the periphery of the tumor (Fig. 6A), but without

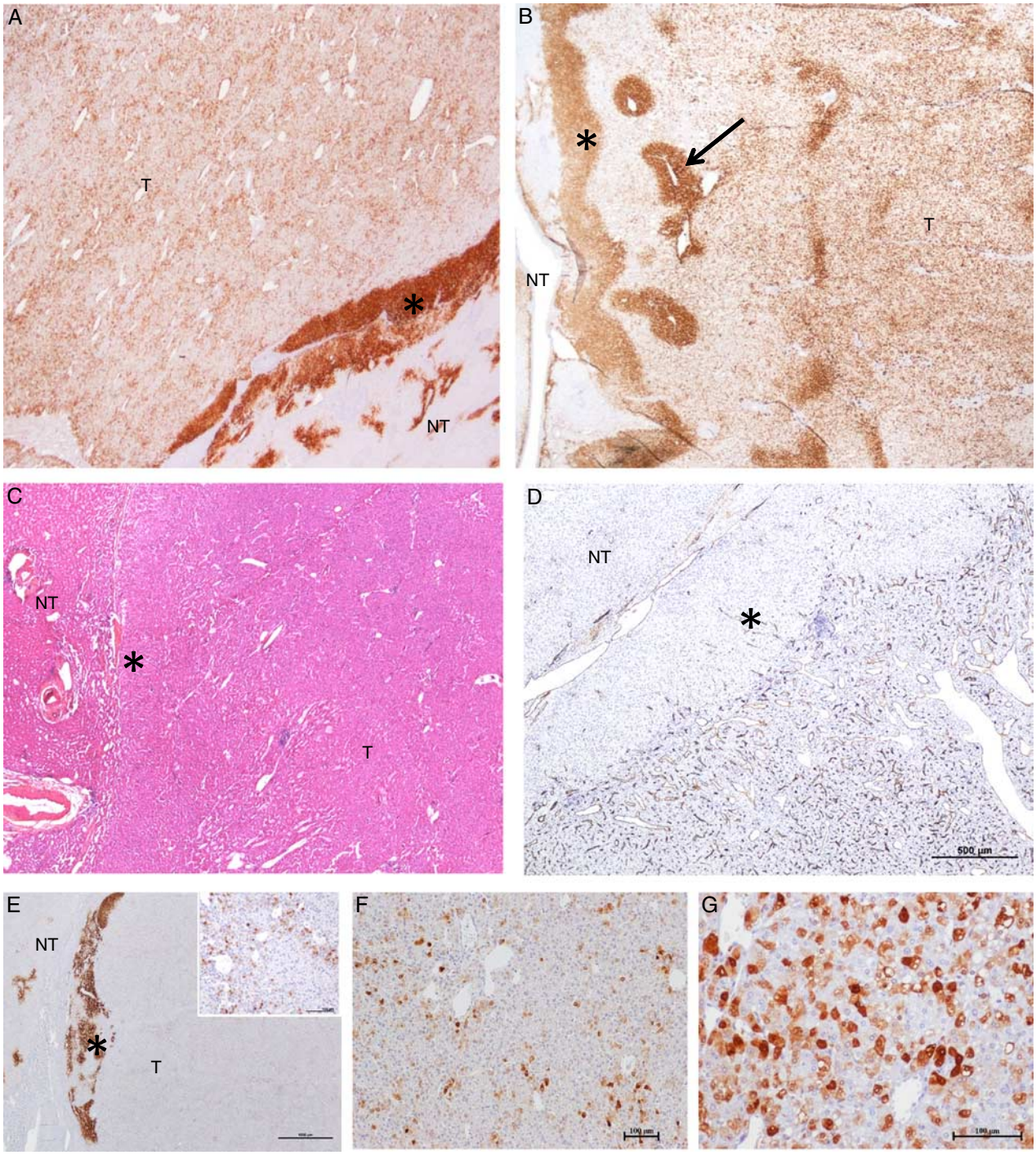

FIGURE 4. Pattern 2: Diffuse heterogenous GS pattern. Case 54 (exon 3 S45 mutated b-HCA) (A) and case 82 (exon 3 S45 mutated b-IHCA) (B). GS staining is diffuse and heterogenous in the tumor (T), associated with a strong positive GS rim (asterisk) at the border area with non tumoral liver (NT). Note in (B) the thick perivascular patches in T (arrow), often observed in the case of IHCA. C and D, Case 41 (b-HCA exon 3 S45). The rim (asterisk) is already vaguely visible at the periphery of T on the hematoxylin and eosin (C), and is further confirmed by its CD34 negativity (asterisk), contrasting with the center of T where CD34 is diffusely expressed in sinusoids (D). E–G, Variations in staining intensity of GS pattern 2: faint GS staining in T (inset), but with a typical rim (asterisk) (E: case 61); moderate intensity (F: case 41); strong intensity (G: case 54).

a well-defined $GS^+/CD34^-$ rim. The CD34 expression was patchy and unremarkable (Fig. 6B). Application of these "negative" criteria resulted in a good interobserver reproducibility (AC1 = 0.74, 95% CI: 0.61-0.88). The sensitivity and specificity of consensus were 87% (95% CI: 69%-96%) and 97% (95% CI: 89%-100%), respectively.

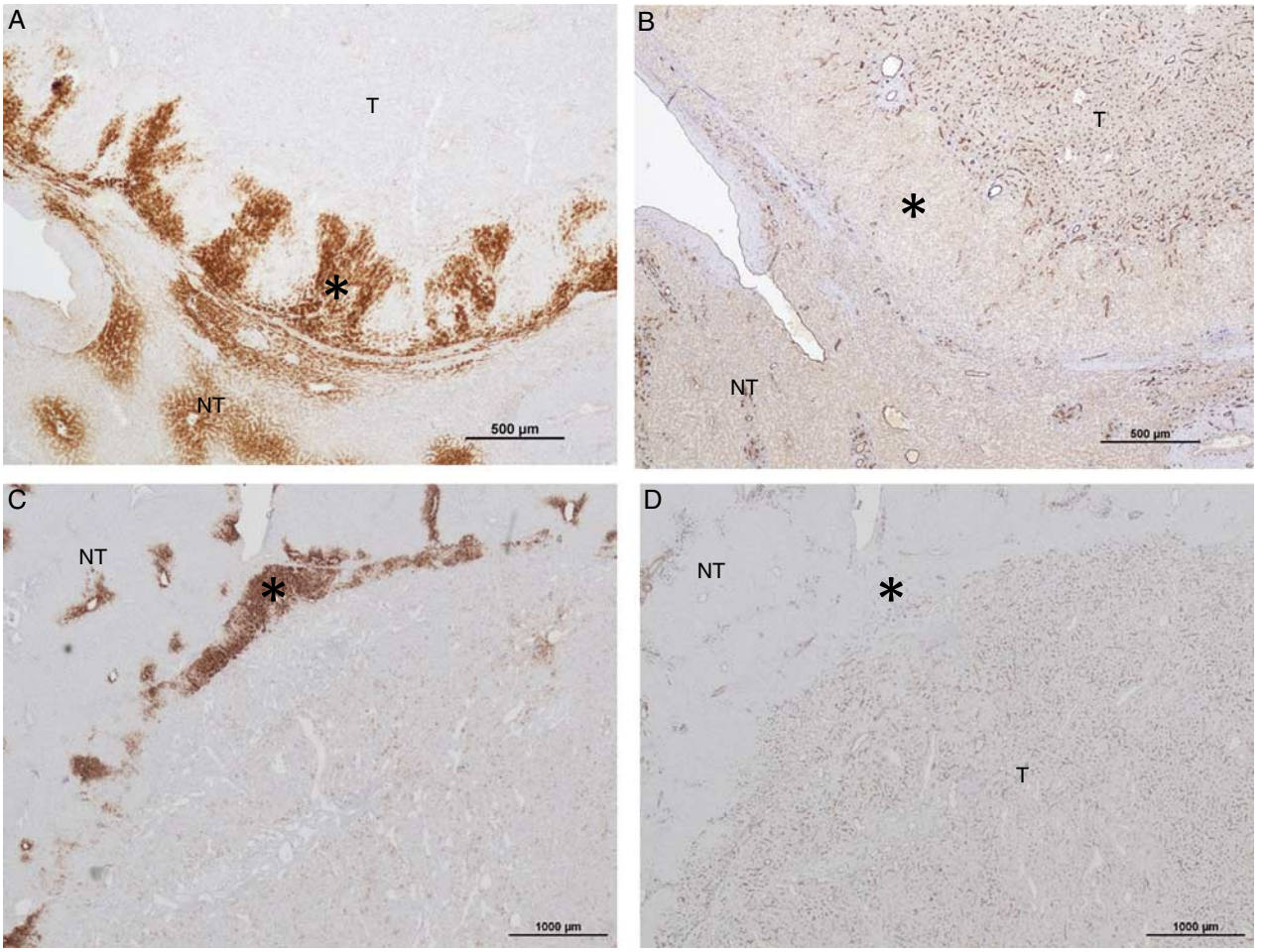

FIGURE 5. Pattern 3: Focal patchy GS pattern. A and B, Case 91 (b-HCA exon 7/8). GS staining, almost absent in the tumor (T), underlines a rim at the periphery of the HCA (asterisk) (A); CD34 is diffuse in the T sinusoids, contrasting with its negativity in the rim (asterisk) (B). C and D, Case 43 (b-HCA exon 7/8). Very faint GS staining in the center of the T associated with a GS+ (C)/CD34– rim (asterisk), contrasting with diffuse CD34 expression in T (D). The faint heterogenous staining of GS within the T may lead to a misinterpretation of pattern 2. NT indicates non tumoral liver.

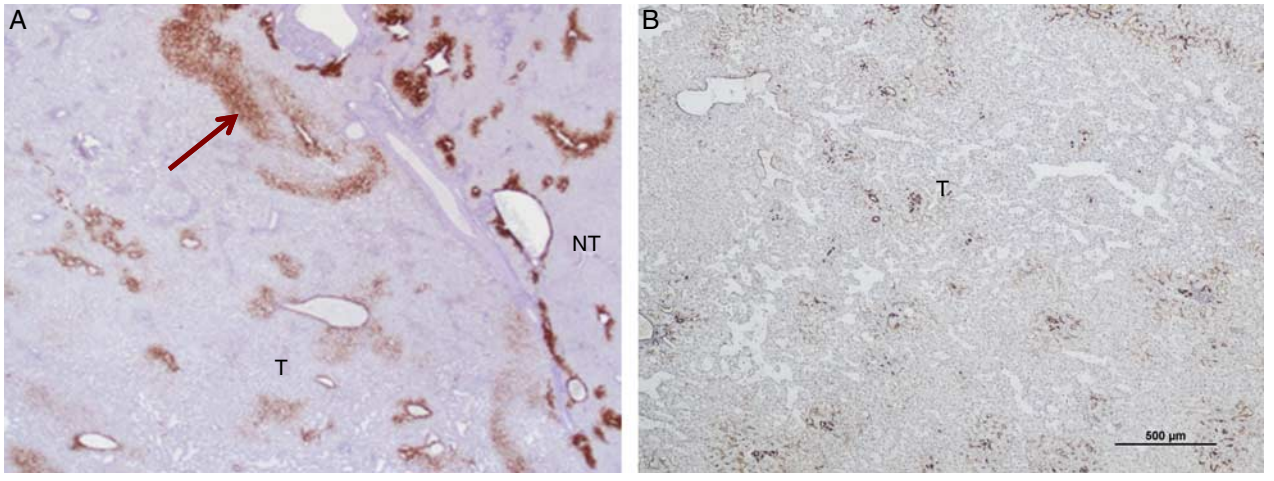

FIGURE 6. IHCA. A and B, Case 67. The tumor (T) contains some GS patches focally reinforced at the periphery of T (arrow), but without a true rim (A); the CD34 sinusoidal staining is unremarkable within T (B). NT indicates non tumoral liver.

TABLE 2. Summary of Statistical Results: Molecular Analysis (Gold Standard) Versus IHC Analysis of Patterns (Consensus)

	95% CI				
Molecular Analysis	**Sensitivity**	**Specificity**	**PPV**	**NPV**	**AUC**
B exon 3 non-S45	0.83 (0.36-0.99)	1.0 (0.96-1.0)	1.0 (0.48-1.0)	0.99 (0.94-1.0)	0.92 (0.75-1.0)
BI exon 3 non-S45	0.80 (0.52-0.96)	1.0 (0.95-1.0)	1.0 (0.74-1.0)	0.96 (0.90-0.99)	0.90 (0.80-1.0)
B exon 3 S45	1.0 (0.75-1.0)	0.93 (0.84-0.97)	0.68 (0.43-0.87)	1.0 (0.95-1.0)	0.96 (0.93-0.99)
BI exon 3 S45	1.0 (0.59-1.0)	0.92 (0.84-0.97)	0.50 (0.23-0.77)	1.0 (0.95-1.0)	0.96 (0.93-0.99)
B exon 7/8	0.55 (0.23-0.83)	1.0 (0.96-1.0)	1.0 (0.54-1.0)	0.94 (0.87-0.98)	0.77 (0.62-0.93)
BI exon 7/8	0.55 (0.23-0.83)	0.96 (0.90-0.99)	0.67 (0.30-0.93)	0.94 (0.87-0.98)	0.75 (0.60-0.91)
IHCA	0.87 (0.69-0.96)	0.97 (0.89-1.0)	0.93 (0.77-0.99)	0.94 (0.85-0.98)	0.92 (0.85-0.98)

AUC indicates area under the curve; B, beta-catenin mutation/deletion; I, inflammatory; NPV, negative predictive value; PPV, positive predictive value.

As mentioned earlier, 3 cases were wrongly interpreted as having exon 7/8 mutation and 1 case as exon 3 S45. However, at reassessment, no fully developed $GS^+/CD34^-$ rim was present, which should have signaled the lack of *CTNNB1* mutation.

When only the total group of inflammatory HCA (IHCA and b-IHCA, n = 63) is considered, the specificity and the sensitivity to predict the presence of a *CTNNB1* mutation was excellent, 87% (95% CI: 69%-96%) and 94% (95% CI: 80%-99%), respectively.

In the assessment of individual evaluations of observers, concordance was present for 66 HCAs (71%), and differences were found in 27 lesions. In 14/27, only 1 observer was divergent, and, at joint reassessment, consensus was reached, leading to a total agreement for 80/93 cases (86%). In 9 of these 80 cases (11%), there was a mismatch with the molecular data. In the 13/93 cases with complete divergent evaluations, the consensus that was reached did not match with the molecular analysis in 9/13 (69%) cases (Table 1). Table 2 summarizes the statistical results.

DISCUSSION

In this multicenter study of GS IHC patterns as a predictive marker for *CTNNB1* exons 3 and 7/8 mutations in 33 b-IHCA and 30 b-HCA with established *CTNNB1* molecular data, we reached excellent levels of interobserver reproducibility and high sensitivity and specificity degrees for mutations of exon 3 non-S45 and exon 3 S45 variants. However, GS IHC alone is not reliable enough to recognize b-(I)HCA with mutation in exon 7/8. This is compensated by our confirmation of the specific feature of the $GS^+/CD34^-$ rim in exon 7/8 and exon 3 S45 mutated b-(I)HCA, which is a valuable aid to recognize that an HCA has an underlying *CTNNB1* mutation.

Pattern 1, the diffuse homogenous GS pattern is specifically associated with exon 3 non-S45 mutation and is recognizable and reproducible in both b-HCA and b-IHCA. Using this pattern an exon 3 non-S45 mutation should not be missed because of the high risk of malignant transformation of this category.

Four cases with exon 3 non-S45 mutations were misdiagnosed as exon 3 S45, but retrospectively, the absence of the $GS^+/CD34^-$ rim and the patchy CD34 central in the lesions should have prevented the misclassification. The variable intensity, yet still diffuse staining also gave the impression of heterogeneity at lower power. This phenomenon may partly be due to a variant hotspot mutation[11] (eg, exon 3 P52S, case 38) and may form a pitfall in this category.

Of note, a small number of HCA cases with strongly and diffusely positive GS but without *CTNNB1* mutation analyzed in FFPE samples have been described.[16,26] This phenomenon can be explained either by known technical issues of molecular analyses,[27] or it might result from the activation of other pathways. Such cases were not included in this study. Nevertheless, a diffuse and strong GS expression in an HCA (b-HCA or b-IHCA) indicates a strong activation of the beta-catenin pathway. As the risk of cancer is linked to the level of beta-catenin activation,[11] such cases should be carefully followed up.

Pattern 2, the diffuse heterogenous GS pattern, is highly reproducible and reliable to identify *CTNNB1* exon 3 S45 mutations for both b-HCA and b-IHCA. Recognition of this mutational subtype is relevant because of its risk of malignant transformation.[2,11,28,29] The reliability in recognizing this diffuse heterogenous pattern (also labeled as "starry sky")[7] whatever the staining intensity (Figs. 4E–G), and its high sensitivity is demonstrated for the first time in this study.

An important finding in this study is the significance of the $GS^+/CD34^-$ rim that indicates the existence of a *CTNNB1* mutation, either exon 3 S45 or exon 7/8. However, this rim does not distinguish between the 2 types of mutations, which can be discriminated by the GS pattern in the central part of the tumor and/or molecular typing. The pathogenetical significance of this rim is not fully understood. We hypothesize that it is most probably related to a difference in vascularization, as also underlined by the sharp CD34 staining distinction between the rim and the center, indicating differences in sinusoidal capillarization. Interestingly, a strong GS^+ hyperplastic area has also been described around some hypervascular malignant primary or secondary liver tumors.[30]

With regard to *pattern 3, the focal patchy GS pattern,* our results show that the identification of exon 7/8 mutation by IHC is of limited reliability. The $GS^+/CD34^-$ rim will indicate an underlying *CTNNB1* mutation (Figs. 5A–D) although confirmation of an exon 7/8 mutation will require molecular typing in 50% of the cases. Establishing exon 7/8 mutation is relevant as the potential for malignant transformation is indeed low but not negligible, as shown in a recent case report.[31] This particular case also had *TERT*

promoter mutation, indicating an additional genetic event contributing to malignant transformation.

The criteria that we have applied in the current study are only applicable in a strict systematic analysis starting by the recognition of the lesion as an HCA and not an HCC because other criteria should be applied for the latter.[32] As the significance of GS expression in the other subtypes of HCA, that is, HNF1α-inactivated HCA and sonic-hedgehog HCA is still unknown, the second step is to subtype the HCA and it is only after this second step that it is possible to proceed with the interpretation of the GS staining together with CD34, as proposed in our algorithm (Fig. 2). Taken together, our results showed that the criteria are applicable to effectively recognize the 2 subtypes of exon 3 mutation in b-(I)HCA, which represent the group with the highest risk of malignant transformation. Of equal clinical importance is our finding that GS staining is also a suitable method to identify the absence of *CTNNB1* mutations in IHCA. Molecular biology remains mandatory in HCA cases showing inconclusive immunohistology.

The strength of our study is that it is strictly based on molecular data. However, there are several limitations. First, we analyzed surgical specimens only, to guarantee the availability of the marginal area between lesional and nonlesional liver. This necessary first step approach means that the applicability of the criteria on biopsy specimens remains to be established. After completion of the study, we assessed the 16 available preresection biopsies (3IHCA, 13 b-(I)HCA) of the current cohort. Our preliminary data in this very limited number of biopsies show that the patterns we described can indeed be discerned in biopsies, especially in the IHCA and exon 3 mutated cases; but, as in the resection specimens, recognition of the exon 7/8 mutated cases was incomplete (data not shown). However, these data are too limited and are also subject to recall bias, to allow application on biopsies at this stage. Such an application will need a prospective and specific biopsy study, with a different larger cohort that should also include focal nodular hyperplasia (FNH) and HCA without *CTNNB1* mutations. With regard to FNH, we can already anticipate the difficult differential diagnosis on a needle biopsy between the GS rim of *CTNNB1* exon 3 S45 and exon 7/8 mutated HCA and the GS map-like pattern of FNH. A second limitation is that the evaluation of the GS immunostaining patterns was performed by expert liver pathologists with long-time experience in HCA analysis and was not compared with the interpretation by general pathologists. However, HCA is a specialized field of medicine, partly due to its rarity, requiring a multidisciplinary approach of specialized teams,[33] including dedicated liver pathologists; hence, our study could be considered as representative.

In conclusion, in an appropriate step-by-step analysis of HCA, recognition of the different GS staining patterns, combined with CD34, is a valuable method to identify the molecular subgroups of *CTNNB1*-mutated HCA at higher risk of malignant transformation, and represents a useful tool for patient management in routine practice. Its application on biopsy samples remains to be validated by a separate study.

ACKNOWLEDGMENTS

The authors acknowledge their colleagues who had performed the molecular analyses: Professor J. Zucman-Rossi and Dr David Cappellen for CHU Bordeaux (Bordeaux, France) and Beaujon Hospital (Paris, France); S. Huitema, Dr M.C. van den Heuvel (for help in selecting cases) and Professor A. van den Berg for University Medical Center Groningen (Groningen, The Netherlands), and Dr B. Bisig and Dr Sc. E. Missiaglia for Lausanne University Hospital (Lausanne, Switzerland), and Dr J. Calderaro for sharing with the authors his experience in GS interpretation. The authors also acknowledge all their clinical colleagues who worked with them in their respective hepatobiliary multidisciplinary teams.

REFERENCES

1. Nault JC, Bioulac-Sage P, Zucman-Rossi J. Hepatocellular benign tumors-from molecular classification to personalized clinical care. *Gastroenterology*. 2013;144:888–902.
2. Nault JC, Couchy G, Balabaud C, et al. Molecular classification of hepatocellular adenoma associates with risk factors, bleeding, and malignant transformation. *Gastroenterology*. 2017;152:880–894.
3. van Rosmalen BV, Coelen RJS, Bieze M, et al. Systematic review of transarterial embolization for hepatocellular adenomas. *Br J Surg*. 2017;104:823–835.
4. Zucman-Rossi J, Jeannot E, Nhieu JT, et al. Genotype-phenotype correlation in hepatocellular adenoma: new classification and relationship with HCC. *Hepatology*. 2006;43:515–524.
5. Stoot JH, Coelen RJ, De Jong MC, et al. Malignant transformation of hepatocellular adenomas into hepatocellular carcinomas: a systematic review including more than 1600 adenoma cases. *HPB (Oxford)*. 2010;12:509–522.
6. Farges O, Ferreira N, Dokmak S, et al. Changing trends in malignant transformation of hepatocellular adenoma. *Gut*. 2011;60:85–89.
7. Bioulac-Sage P, Kakar S, et al. Hepatocellular adenoma. In: WHO Classification of Tumours, ed. *Digestive System Tumours*, 5th edition. Lyon, France: International Agency for Research on Cancer (IARC) Press; 2019:224–228.
8. Sempoux C, Paradis V, Komuta M, et al. Hepatocellular nodules expressing markers of hepatocellular adenomas in Budd-Chiari syndrome and other rare hepatic vascular disorders. *J Hepatol*. 2015;63:1173–1180.
9. Gupta S, Naini BV, Munoz R, et al. Hepatocellular neoplasms arising in association with androgen use. *Am J Surg Pathol*. 2016;40:454–461.
10. Jang HJ, Yang HR, Ko JS, et al. Development of hepatocellular carcinoma in patients with glycogen storage disease: a single center retrospective study. *J Korean Med Sci*. 2020;35:e5.
11. Rebouissou S, Franconi A, Calderaro J, et al. Genotype-phenotype correlation of CTNNB1 mutations reveals different b-catenin activity associated with liver tumor progression. *Hepatology*. 2016;64:2047–2061.
12. Saldarriaga J, Bisig B, Couchy G, et al. Focal β-catenin mutation identified on formalin-fixed and paraffin-embedded inflammatory hepatocellular adenomas. *Histopathology*. 2017;71:989–993.
13. Torbenson M, Lee JH, Choti M, et al. Hepatic adenomas: analysis of sex steroid receptor status and the Wnt signaling pathway. *Mod Pathol*. 2002;15:189–196.
14. Bioulac-Sage P, Rebouissou S, Thomas C, et al. Hepatocellular adenoma subtype classification using molecular markers and immunohistochemistry. *Hepatology*. 2007;46:740–748.
15. Bioulac-Sage P, Sempoux C, Frulio N, et al. Snapshot summary of diagnosis and management of hepatocellular adenoma subtypes. *Clin Res Hepatol Gastroenterol*. 2019;43:12–19.
16. Hale G, Liu X, Hu J, Xu Z, et al. Correlation of exon 3 β-catenin mutations with glutamine synthetase staining patterns in hepatocellular adenoma and hepatocellular carcinoma. *Mod Pathol*. 2016;29:1370–1380.
17. Kakar S, Ferrell LD. Glutamine synthetase staining and CTNNB1 mutation in hepatocellular adenomas. *Hepatology*. 2017;66:2092–2093.
18. Rebouissou S, Bioulac-Sage P, Nault JC, et al. Genotype-phenotype correlation of CTNNB1 mutations reveals different b-catenin activity associated with liver tumor progression. *Hepatology*. 2017;66:2093–2094.

19. Bioulac-Sage P, Sempoux C, Balabaud C. Hepatocellular adenoma: classification, variants and clinical relevance. *Semin Diagn Pathol*. 2017;34:112–125.
20. Cappellen D, Balabaud C, Bioulac-Sage P. A difficult case of β-catenin-mutated hepatocellular adenoma: a lesson for diagnosis. *Histopathology*. 2019;74:355–357.
21. Bioulac-Sage P, Cubel G, Balabaud C, et al. Revisiting the pathology of resected benign hepatocellular nodules using new immunohistochemical markers. *Semin Liver Dis*. 2011;31:91–103.
22. Putra J, Ferrell LD, Gouw ASH, et al. Malignant transformation of liver fatty acid binding protein-deficient hepatocellular adenomas: histopathologic spectrum of a rare phenomenon. *Mod Pathol*. 2020;33:665–675.
23. Sala M, Gonzales D, Leste-Lasserre T, et al. ASS1 overexpression: a hallmark of sonic hedgehog hepatocellular adenomas; recommendations for clinical practice. *Hepatol Commun*. 2020;4:809–824.
24. Wongpakaran N, Wongpakaran T, Wedding D, et al. A comparison of Cohen's kappa and Gwet's AC1 when calculating inter-rater reliability coefficients: astudy conducted with personality disorder samples. *BMC Med Res Methodol*. 2013;13:61.
25. Shankar V, Bangdiwala SI. Observer agreement paradoxes in 2×2 tables: comparison of agreement measures. *BMC Med Res Methodol*. 2014;14:100.
26. Longerich T, Endris V, Neumann O, et al. RSPO2 gene rearrangement: a powerful driver of β-catenin activation in liver tumours. *Gut*. 2019;68:1287–1296.
27. Bayard Q, Nault J-C, Zucman-Rossi J. RSPO2 abnormal transcripts result from read-through in liver tumors with high beta-catenin activation and CTNNB1 mutations. *Gut*. 2020;69:1152–1153.
28. Sempoux C, Bisig B, Couchy G, et al. Malignant transformation of a β-catenin inflammatory adenoma due to an S45 β-catenin-activating mutation present 12 years before. *Hum Pathol*. 2017;62:122–125.
29. Vilarinho S, Erson-Omay EZ, Mitchell-Richards K, et al. Exome analysis of the evolutionary path of hepatocellular adenoma-carcinoma transition, vascular invasion and brain dissemination. *J Hepatol*. 2017;67:186–191.
30. Arnason T, Fleming KE, Wanless IR. Peritumoral hyperplasia of the liver: a response to portal vein invasion by hypervascular neoplasms. *Histopathology*. 2013;62:458–464.
31. Klompenhouwer AJ, Thomeer MGJ, Dinjens WNM, et al. Phenotype or genotype: decision-making dilemmas in hepatocellular adenoma. *Hepatology*. 2019;70:1866–1868.
32. Nguyen TB, Roncalli M, Di Tommaso L, et al. Combined use of heat-shock protein 70 and glutamine synthetase is useful in the distinction of typical hepatocellular adenoma from atypical hepatocellular neoplasms and well-differentiated hepatocellular carcinoma. *Mod Pathol*. 2016;29:283–292.
33. Blanc JF, Frulio N, Chiche L, et al. Hepatocellular adenoma management: call for shared guidelines and multidisciplinary approach. *Clin Res Hepatol Gastroenterol*. 2015;39:180–187.